Net Load Forecast Error Compensation for Peak Shaving in a Grid-Connected PV Storage System

Rampelli Manojkumar, *Member, IEEE*, Chandan Kumar, *Senior Member, IEEE*, Sanjib Ganguly, *Senior Member, IEEE*, and João P. S. Catalão, *Fellow, IEEE*

***Abstract*—In modern power systems, it is important to compensate net load forecast errors which are caused due to variability and uncertainty of load and renewable energy source powers for improving the stability and reliability. Super capacitor (SC) is a well suited component for compensating forecast error due to its power and energy density characteristics. In this article, a novel method is proposed for net load forecast error compensation through SC application. The proposed method is simple and general which can be used at industry scale while implementing the energy management applications. In order to test the performance of the proposed method, a grid-connected photovoltaic storage system is considered. The forecast error in load/PV powers is compensated while limiting both grid demand and feed-in powers to their optimal limits. Battery energy storage system charge/discharge schedules are controlled by a rule-based peak shaving method to minimize the day-ahead average peak demand of the system. For controlling SC charge/discharge schedules, the proposed net load forecast error compensation method is used. It is observed that the peak demand and feed-in powers are reduced significantly with the proposed method as compared with the case when there is no net load forecast error compensation.**

***Index Terms*—Battery energy storage, demand and feed-in limits, peak shaving, renewable energy sources, super capacitor**

NOMENCLATURE

A. Notations

$\eta_{bc}\{\eta_{bd}\}$	Battery charge{discharge} efficiency
C	Capacitance of SC
E^*_{bd}	Dischargeable energy of the battery
E^i_{sc}	Initial estimate of SC energy
$E_{bc}\{E_{bd}\}$	Energy needed to charge{to be discharged by} the battery over a day
E_{br}	Battery energy rating
$E_{nlfc}\{E_{gc}\}$	Available net load feed-in{grid} energy to charge the battery over a day
E_{sc}	Energy of SC
P^i_{sc}	Initial estimate of SC power
$P^l_{bc}\{P^l_{bd}\}$	Charge{discharge} power limit of battery
P^{nv}_{g-peak}	Peak grid power over a day when there is no forecast error
$P^{nv}_g(t)$	Grid power when there is no forecast error
$P_{bc}\{P_{bd}\}$	Battery charge{discharge} powers
$P_b\{P_g\}$	Battery{grid} power
P_{dl}	Demand limit
P_{fil}	Feed-in limit
$P_l\{P_{pv}\}$	Load{PV} power
$P_{nld}\{P_{nlf}\}$	Net load demand{feed-in} power
$P_{nlfc-b}\{P_{gc-b}\}$	Net load feed-in{grid} power used to charge the battery
$P_{nlfc}\{P_{gc}\}$	Available net load feed-in{grid} power to charge the battery
P_{nlfe}	Net load forecast error
P_{nl}	Net load power
P_{scr}	Rated power limit of SC
P_{sc}	Power of SC
$SoC_{b-i}\{SoC_{b-f}\}$	Battery SoC at the start{end} of the day
$SoC_{bl}\{SoC_{bu}\}$	Battery SoC lower{upper} limit
$SoC_b\{SoC_{sc}\}$	SoC of the battery{SC}
SoC_{sc-i}	SoC of SC at the start of the day
$SoC_{scl}\{SoC_{scu}\}$	SC SoC lower{upper} limit
T	Total predictive horizon
t	Time
T_r	Each time slot duration
t_1	Time slots when net load feed-in power to charge the battery is more than the feed-in limit
t_d, t_c	Discharge mode, charge mode times
V_{br}	Voltage rating of the battery
V_{scr}	Nominal voltage of SC
V_{sc}	Open circuit voltage of SC
P_{l-r}	Rated load power
P_{pv-ins}	PV source installed power
P_{gd}	Grid demand power
P_{gf}	Grid feed-in power
P_{gd-p}	Peak grid demand power
P_{gf-p}	Peak grid feed-in power
R_{lfe}	Load forecast error range
R_{pvfe}	PV power forecast error range

B. Indices

f	Index of average hourly forecast values
o	Index of optimal value

Manuscript received January 22, 2023; revised May 10, 2023, July 11 2023; accepted September 17, 2023. *(Corresponding author: Rampelli Manojkumar).*

Rampelli Manojkumar is with the Department of Electrical and Electronics Engineering, BVRIT HYDERABAD College of Engineering for Women, Hyderabad, 500090, India (e-mail: manoj023manoj@gmail.com).

Chandan Kumar, and Sanjib Ganguly are with the Department of Electronics and Electrical Engineering, Indian Institute of Technology Guwahati, Guwahati 781039, India (e-mail: chandank@iitg.ac.in; sganguly@iitg.ac.in).

João P. S. Catalão is with the Faculty of Engineering of the University of Porto and INESC TEC, Porto 4200-465, Portugal (e-mail:catalao@fe.up.pt).

I. Introduction

The net load forecasts help power system operators in optimizing power generation, reduce the need for backup power, and improve the overall performance of the power system. However, the errors associated with the net load forecasts are unavoidable due to the reasons such as uncertainty in end user behavior as well as weather conditions, and data limitation [1]. Therefore, it is important to consider the net load forecast errors in power systems planning and operation to ensure grid stability, frequency regulation, reliability, and cost-effectiveness [2], [3]. Moreover, the net load forecasts are used for implementing energy management applications which help in distributed energy resource scheduling, energy market operation, etc [4]. These net load forecast errors are mainly due to variability and uncertainty of load and renewable energy powers such as photovoltaic (PV) powers, etc. The difference between minutely power and hourly average power is defined as variability whereas the difference between the hourly average forecast power and hourly average power is defined as uncertainty [5]. With this variability and uncertainty, the net load power varies for every 5 to 15 minutes of the day [6]. There are several techniques used for net load forecast error compensation in the existing literature such as model predictive control [7], neural networks [8]. Further, it is possible to compensate the net load forecast errors using flexible loads and energy storage devices [9]–[11].

In [10], [11], the size of energy storage devices is optimized while compensating the forecast error of wind power. However, the drawback in those works is that the particular energy storage device type and its modelling details are not discussed. In [12], the battery energy storage devices are considered and their size is optimized while minimizing the forecast errors of wind power. However, the drawback is that if the battery is used for charging and discharging with respect to minutely variation of net load power, its lifetime is reduced. In general, the super capacitor (SC) is used along with the battery to absorb the transients/ripples during load changes to increase the lifetime of the battery [13], [14]. The conventional SC is a high power and low energy density device [15]. Considering the minutely variation of net load power, it is difficult to use conventional SC for compensating the forecast error due to their low energy density ratings. However, a hybrid SC with high energy density rating can be used for compensating forecast error [16]. In the existing literature of net load forecast error compensation [7]–[12], the application of SC for net load forecast error compensation is not discussed. In order to fill this research gap, a generalized net load forecast error compensation method is proposed in this paper specifically using SC which can be applied for real-time implementation of any energy management application involving net load forecasts. The various methods/devices used for net load forecast error compensation are given in Table I.

Further, in this article, in order to know the impact of proposed method, a grid-connected PV-BESS system is chosen where BESS is used for peak shaving application. Peak shaving is chosen as it is an important energy management application which provides several benefits to energy consumers as well as to grid operators [17]. Peak shaving improves load factor and helps in achieving economical operation of generation [18]. It is also helpful for increasing the efficiency and for reducing consumers energy costs [19]. Moreover, peak shaving is useful for better voltage profile in distribution networks [20]. In [21], the implementation of a computational method to minimize the peak power consumption is discussed. In [22], a heuristic algorithm known as MinPeak is formulated to reduce the peak demand. However, the energy storage is not used for the peak shaving application. In [23], an attempt is made to reduce the peak power through the determination of the discharge quantity of energy storage. In [24], the peak shaving is done while minimizing the operating costs of the system where the trajectory of state of charge (SoC) of the battery is considered as one of the control variables. This leads to twenty four control variables over a day with hourly dispatch of the battery. Further, the peak shaving application via demand/feed-in power limits with the help of the battery energy storage systems (BESS) is presented in literature. In [25]–[28], only the demand limit (DL) is considered, but not the feed-in limit (FIL). The significance of FIL for voltage profile improvement in distribution systems is discussed in [29]. The consideration of FIL avoids voltage rise issues and also increases the efficiency of the system.

Recently, a peak shaving method is proposed in [30] through rule-based approach which is the suggested approach by IEEE Std 2030.7 [32] for microgrid control purpose due to their advantages like easy implementation, easy maintenance, clear meaning of the chosen rules, and low cost. The proposed method in [30] considered both DL and FIL. However, this method does not consider the round-trip efficiency of battery and its power limits. Moreover, the load and PV powers are used as separate inputs for deciding the battery modes which leads to the complexity of peak shaving method (two different charge modes and more number of rules). To avoid these limitations, the rule-based method is improved while addressing the modelling issues of battery and considering the only one input i.e., the net power at a particular node in [31]. However, the forecast errors of load and PV power are not considered for real time implementation. In order to fill this research gap, the proposed net load forecast error compensation method is applied in the considered grid-connected PV-BESS system and its impact on peak shaving operation is analysed. The qualitative comparison of existing works with proposed method based on peak shaving method and consideration of forecast error compensation is given in Table II.

TABLE I
Methods/Devices Used for Net Load Forecast Error Compensation

Reference	Method/device used for net load forecast error compensation
[7]	Model predictive control
[8]	Artificial neural networks
[9]	Flexible loads
[10], [11]	Energy storage devices
[12]	BESS
Proposed	SC

TABLE II
QUALITATIVE COMPARISON BASED ON PEAK SHAVING METHODS AND CONSIDERATION OF NET LOAD FORECAST ERROR COMPENSATION

Reference	Method of peak shaving operation	Forecast error compensation
[21]	Electric vehicle (EV) charging control	✓
[22]	Appliances scheduling	×
[23]	Energy storage discharging control	×
[24]	Coordination of distributed generators, BESSs, and voltage regulating devices	✓
[25]	Coordination of PVs, BESSs, and EVs	×
[26]	Utilization of energy storage systems and real time thermal ratings	×
[27]	Scheduling of BESSs	×
[28]	Appliances scheduling considering DL	×
[29]	Feed-in power limitation	×
[30], [31]	Optimized rule-based approach considering both DL and FIL	×
Proposed	Optimized rule-based approach considering both DL and FIL	✓

The overall contributions of the paper are given as follows.

1) To propose a net load forecast error compensation method using SC considering net load forecast error as input.
2) To apply the proposed forecast error compensation method in a grid connected PV storage system to know its impact on peak shaving operation.

The organization of the paper is as given here. Section II presents the overview of proposed control method. Section III discusses the peak shaving method. Section IV describes the proposed net load forecast error compensation method using SC. The simulation results and conclusions are presented in Section V and VI, respectively.

II. OVERVIEW OF PROPOSED CONTROL

The proposed method needs to be tested at a generalized point of common coupling (PCC) or node of a system. If the proposed method performs effectively at a generalized node, it can be applied at any node in a power system irrespective of the size of the system. Therefore, in this work a grid-connected system consisting of load, PV source, the battery, and SC is considered as shown in Fig. 1 [13]. The load is connected at the ac bus of the system. The normalized average hourly day-ahead load power profile with respect to its peak value is shown in Fig. 2 [30]. The PV source is connected to dc bus via a dc/dc converter. The normalized average hourly day-ahead PV power profile with respect to its peak value is shown in Fig. 2 [33]. The battery is connected at dc bus via a dc/dc converter which is used for peak shaving operation. The SC is connected at the dc bus via a dc/dc converter which is used for compensating forecast error in load and PV powers.

The overview of proposed control for the considered system is given in Fig. 3. As per the proposed control, the real time net load power is used to decide charge/discharge schedules of the battery and SC. The net load is considered to be varying for each 5 minutes as per [6]. However, it is to be noted that the battery powers are controlled for each one hour considering the day ahead hourly average power profiles to reduce the number of charge and discharge cycles of the battery over a day which in turn results in the increased life time of the battery. Accordingly, the net load power is expressed as sum of its average hourly net load power forecast and forecast error as given in (1).

$$P_{nl}(t) = P^{f}_{nl}(t) + P_{nlfe}(t) \tag{1}$$

where 't' implies the time slot $[(t-1)\times T_r, t\times T_r]$ and T_r is chosen as 5 minutes. The forecast error is the sum of variability and uncertainty of net load power.

The net load power is considered as difference between the load power and PV powers as given in (2),

$$P_{nl} = P_l - P_{pv}. \tag{2}$$

Further, the average hourly net load power forecasts which are positive over the day are considered as net load demand powers as given in (3).

$$\begin{aligned} P^{f}_{nld}(t) &= P^{f}_{nl}(t),\ P^{f}_{nl} > 0 \\ &= 0,\ \text{otherwise.} \end{aligned} \tag{3}$$

The net load power forecasts which are negative are considered as net load feed-in power as given in (4).

$$\begin{aligned} P^{f}_{nlf}(t) &= -P^{f}_{nl}(t),\ P^{f}_{nl} \leq 0 \\ &= 0,\ \text{otherwise.} \end{aligned} \tag{4}$$

The proposed peak shaving method provides the battery schedules using average day-ahead hourly net load power forecasts as input. The net load forecast error compensation method provides SC charge/discharge schedules using net load forecast error as input. In order to implement the proposed control, the dc/dc converters of battery and SC are operated in current control mode for supplying the required charge/discharge power to the dc bus of the system.

III. PEAK SHAVING METHOD

The battery charge/discharge schedules are optimally controlled based on peak shaving method which is presented in this section [31]. The objective of the peak shaving method is to minimize the peak demand over a day considering the day-ahead forecasts of that particular day. In this scenario, there exists a certain dischargeable energy of battery which can limit the peak demand of the day to a certain value i.e., DL for any given day based on the available renewable energy and the load demand. Therefore, the DL is considered as constant for a particular day. Based on the DL, the discharge and charge modes of the battery are decided as discussed follows.

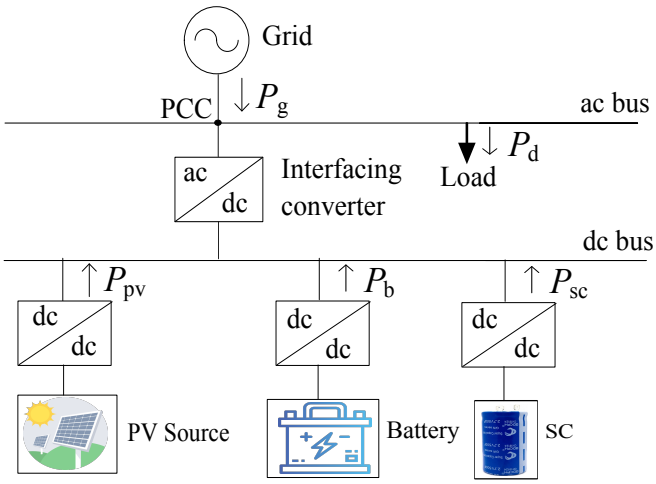

Fig. 1. Considered grid connected PV hybrid storage system.

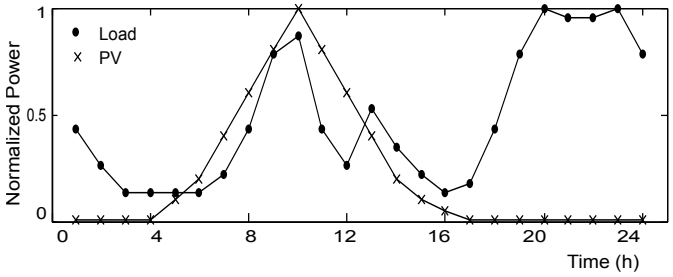

Fig. 2. Normalized day-ahead load demand and PV power forecasts profiles [30], [33].

A. Discharge and Charge Modes of the Battery

The modes of battery are chosen to limit grid power to DL considering there is no forecast error.

1) *Discharge Mode:* When the net load demand forecast is more than DL i.e., $P^f_{nld}(t) > P_{dl}$, the battery is discharged so that the grid power demand is limited to DL.
2) *Charge Mode:* When the net load demand forecast is less than or equal to DL i.e., $P^f_{nld}(t) \leq P_{dl}$, the battery is charged.

B. Control Inputs

The control inputs are obtained using the net load power forecasts. These inputs are DL, energy needed to charge the battery, available net load feed-in energy to charge the battery, available grid energy to charge the battery, coefficient of grid energy to charge the battery, and FIL. The order of calculating the inputs is given in Fig. 4. The determination of these inputs is explained as follows:

1) Demand Limit: The DL is determined considering that the energy to be discharged from battery must be equal to the battery dischargable energy which is given as

$$E_{bd} = E^*_{bd} \tag{5}$$

where E^*_{bd} is the chosen control variable which is determined optimally.

During discharge mode, the battery is used to provide required power i.e., $(P^f_{nld}(t) - P_{dl})$ for limiting $P^{nv}_g(t)$ to P_{dl}. However, with the discharge power limit (P^l_{bd}), the battery discharge power is calculated as

$$\begin{aligned} P_{bd}(t) &= (P^f_{nld}(t) - P_{dl})/\eta_d, (P^f_{nld}(t) - P_{dl}) \leq P^l_{bd} \\ &= P^l_{bd}, (P^f_{nld}(t) - P_{dl}) > P^l_{bd} \end{aligned} \tag{6}$$

Then E_{bd} is determined as

$$E_{bd} = \sum_{t=1}^{T} P_{bd}(t). \tag{7}$$

From (5),

$$\sum_{t=1}^{T} P_{bd}(t) - E^*_{bd} = 0. \tag{8}$$

Equation (8) is in the form of $f(P_{dl}) = 0$. To solve for P_{dl}, the regula falsi method is used [30].

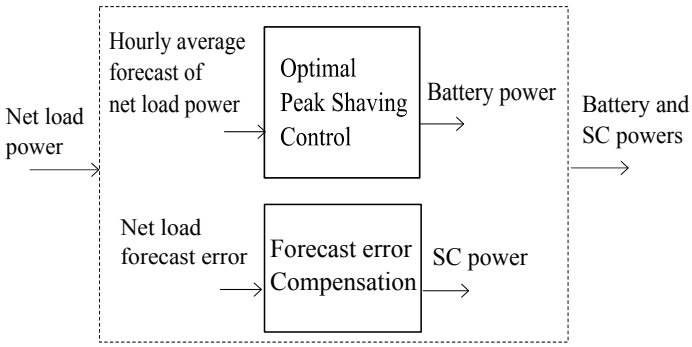

Fig. 3. Overview of proposed control.

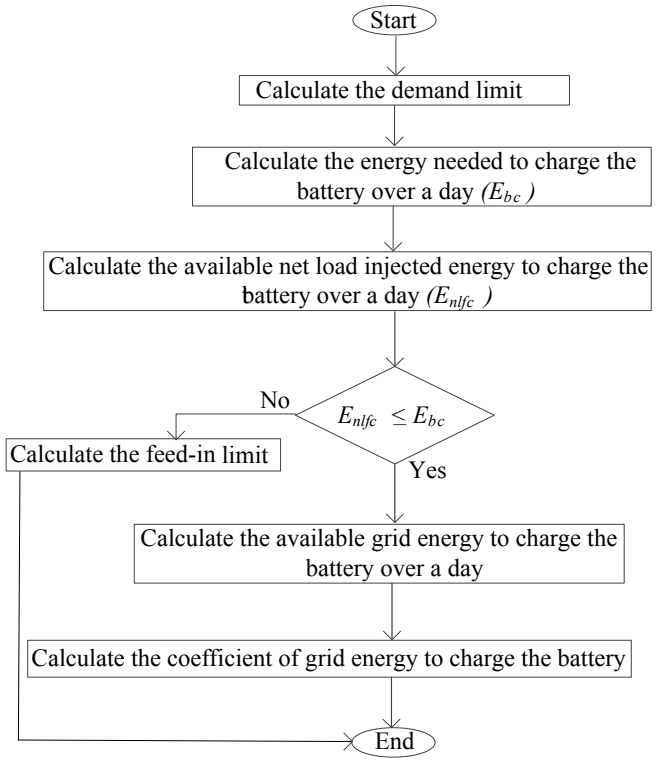

Fig. 4. Order of calculating control inputs of peak shaving method.

2) Energy Needed to Charge the Battery: The state of charge (SoC) at the end of the day must be equal to the SoC of starting of the day for flexible day-to-day management. For that, E_{bc} should be the same as E_{bd} i.e.,

$$E_{bc} = E_{bd} = E^*_{bd}. \tag{9}$$

3) Available Net Load Feed-in Energy to Charge the Battery: Battery has to be charged by E_{bc} using either net load feed-in power or grid power. Firstly, available net load feed-in energy to charge the battery (without sending to grid) is calculated. During t_c, P^f_{nlf} is available to charge the battery. By considering the charging power limit, available net load feed-in power for charging the battery is given in (10),

$$\begin{aligned} P_{nlfc}(t) &= P^f_{nlf}(t), P^f_{nlf}(t) \leq P^l_{bc} \\ &= P^l_{bc}, P^f_{nlf}(t) > P^l_{bc}. \end{aligned} \tag{10}$$

Then E_{nlfc} is given as

$$E_{nlfc} = \sum_{t=1}^{T} P_{nlfc}(t). \tag{11}$$

4) Available Grid Energy to Charge the Battery: When $E_{nlfc} < E_{bc}$, the energy required to complete the battery charging is supplied by grid. As the grid power should be limited to P_{dl}, the available grid power to charge the battery is calculated as

$$\begin{aligned} P_{gc}(t) &= P_{dl} - P^f_{nld}(t), \forall t \in t_c \\ &= 0, \text{ otherwise.} \end{aligned} \tag{12}$$

Then E_{gc} is determined using (13),

$$E_{gc} = \sum_{t=1}^{T} P_{gc}(t). \tag{13}$$

5) Coefficient of Grid Energy to Charge the Battery: When $E_{nlfc} < E_{bc}$, the grid power is used to charge the battery for supplying remaining $E_{bc} - E_{nlfc}$ over a day. Considering C_g as the fraction of the grid energy required to completely charge the battery, it is determined as given in (14),

$$\begin{aligned} C_g E_{gc} &= E_{bc} - E_{nlfc} \\ C_g &= \frac{E_{bc} - E_{nlfc}}{E_{gc}}. \end{aligned} \tag{14}$$

6) Feed-in Limit: If $E_{nlfc} \geq E_{bc}$, P_{fil} is determined such that the battery is completely charged with $P_{nlfc}(t) - P_{fil}$ when $P_{nlfc}(t) > P_{fil}$. It means that the available net load feed-in power to charge the battery is not used when $P_{nlfc}(t) \leq P_{fil}$ i.e.,

$$\sum (P_{nlfc}(t) - P_{fil}) = E_{bc}, \forall t \in t_c \&\& t_1 \tag{15}$$

where symbol '&&' is logical AND operator. Then,

$$\sum (P_{nlfc}(t) - P_{fil}) - E_{bc} = 0, \forall t \in t_c \&\& t_1. \tag{16}$$

Equation (16) is in form of $f(P_{fil}) = 0$. It is solved using the regula falsi method [30].

Now, the proposed rules for peak shaving method and determination of optimal control inputs are discussed as follows.

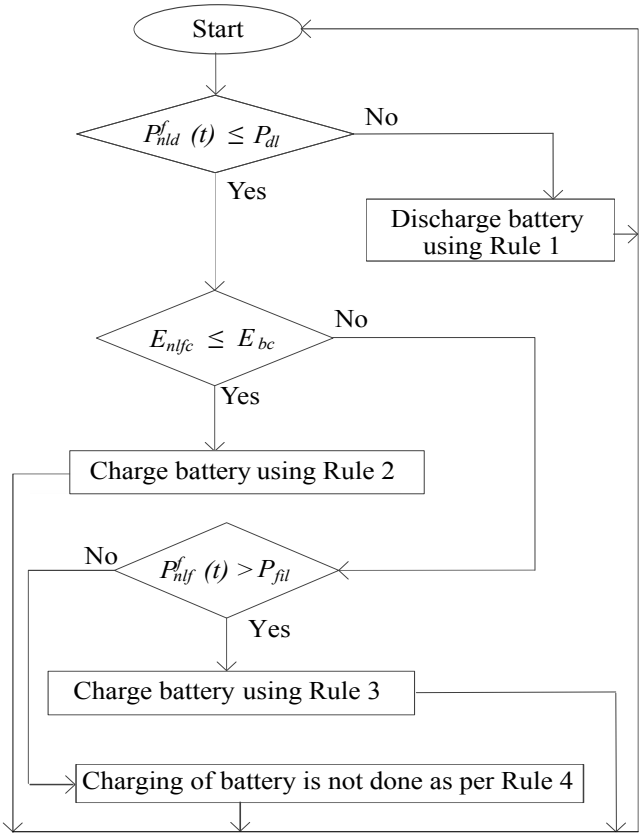

Fig. 5. Peak shaving algorithm.

C. Proposed Rules for Peak Shaving Method

The rules for peak shaving are formulated such that the day-to-day management is flexible while limiting grid power to DL and FIL.

Rule 1: Battery is discharged during t_d by $P_{bd}(t)$ amount of power.

Rule 2: During t_c, if $E_{nlfc} \leq E_{bc}$ both the net load feed-in power and grid power are used for charging battery. The net load feed-in power used for charging battery i.e., $P_{nlfc-b}(t) = P_{nlfc}(t)$ and grid power used for charging the battery i.e., $P_{gc-b}(t) = C_g P_{gc}(t)$ as per (10) and (14). Then, charging power of battery is $P_{bc}(t) = P_{nlfc-b}(t) + P_{gc-b}(t)$

Rule 3: During t_c, if $E_{nlfc} > E_{bc} \&\& P_{nlfc}(t) > P_{fil}$, the grid power is not used to charge the battery. The net load feed-in power is used for charging the battery according to (10). It means that $P_{bc}(t) = P_{nlfc-b}(t) = P_{nlfc}(t) - P_{fil}$.

Rule 4: During t_c, if $E_{nlfc} > E_{bc} \&\& P_{nlfc}(t) \leq P_{fil}$, both the grid and net load feed-in power are not used for charging the battery. Therefore $P_{bc}(t) = 0$.

Fig. 5 shows the procedure of determining battery schedules with the help of the presented rules. Note that the coulomb-counting method is used to determine the SoC of the battery while implementing the proposed peak shaving method [33].

D. Optimal Control Inputs

The peak shaving method is optimized with optimal control inputs which are calculated as discussed in this section. The

fitness function and constraints of the chosen optimization problem are given in (17)-(22),

$$\text{minimize} \quad f = P^{nv}_{g-peak}. \tag{17}$$

subjected to

1) Power balance constraint

$$P^{nv}_{g}(t) + P_b(t) = P^{f}_{nl}(t). \tag{18}$$

2) Battery SoC Constraints

$$SoC_{bl} \leq SoC_b(t) \leq SoC_{bu}, SoC_{b-f} = SoC_{b-i}. \tag{19}$$

3) Constraints of charge and discharge power of battery

$$P_{bc}(t) \leq P^{l}_{bc}, P_{bd}(t) \leq P^{l}_{bd}. \tag{20}$$

4) Constraint of energy capacity of battery

$$E^{*}_{bd} \leq E_{br}. \tag{21}$$

5) Available grid and PV energy constraint to charge battery

$$E_{gc} + E_{nlfc} \geq E_{bc} \tag{22}$$

The battery power considering charge/discharge efficiency is determined as

$$\begin{aligned} P_b(t) &= P_{bc}(t)/\eta_c, \text{ during charging} \\ &= P_{bd}(t) \times \eta_d, \text{ during discharging.} \end{aligned} \tag{23}$$

Note that there is no SC power in (18) because the SC and the battery are independently controlled as per proposed method. The E^{*}_{bd} is chosen as the decision variable, since the required control inputs for peak shaving are the functions of E^{*}_{bd}. It is chosen between 0 kWh and energy rating of the battery.

$$0 \leq E^{*}_{bd} \leq E_{br}. \tag{24}$$

The fitness function is non-linear. Since the genetic algorithm (GA) is the widely used optimization technique for solving non-linear problems, the GA solver used for solving the optimization problem. The default values are chosen as per GA solver of MATLAB for parameters of, etc. However, the population size is tuned such that multiple runs provide almost equal best fitness values. Because the population size is an important parameter of GA on which the convergence and operating time of GA depends on. Accordingly, a population size of 20 is considered such that several runs converges to values which are close to each other.

IV. Proposed Net Load Forecast Error Compensation Method Using SC

The SC is used to compensate the forecast error while considering its SoC and rated power constraints. The SoC and energy of SC are determined as given in (25) and (26), respectively [34].

$$SoC_{sc} = \frac{V_{sc}}{V_{scr}} \tag{25}$$

$$E_{sc} = \frac{1}{2} C V^2_{sc} \tag{26}$$

From (25) and (26), the E_{sc} is

$$E_{sc} = \frac{1}{2} C (SoC_{sc} V_{scr})^2. \tag{27}$$

The (27) shows that the energy stored in SC is proportional to the square of its SoC. It means that there will be lower and upper limits of E_{sc} corresponding to the lower and upper limits of SoC. Therefore, the energy stored in capacitor must be within its limits in order to satisfy SoC constraints. Further, the SC power must be within its rated power limit. Considering these constraints the SC power is determined. The proposed SC control is shown as flowchart in Fig. 6 and explained as follows.

A. SC Power During Discharging

The SC is discharged when net load forecast error is greater than zero. Firstly an initial estimate of SC power is determined considering energy storage and rated power constraints as given in (28),

$$\begin{aligned} P^{i}_{sc}(t) &= 0, E_{sc}(t-1) = E_{scl} \\ &= P_{scr}, E_{sc}(t-1) \neq E_{scl} \&\& P_{nlfe}(t) > P_{scr} \\ &= P_{nlfe}, E_{sc}(t-1) \neq E_{scl} \&\& P_{nlfe}(t) \leq P_{scr}. \end{aligned} \tag{28}$$

It means that if the available energy in SC is at its lower limit, the SC is not discharged. Otherwise, it is discharged either by P_{scr} if $P_{nlfe}(t) > P_{scr}$ or by $P_{nlfe}(t)$ if $P_{nlfe}(t) \leq P_{scr}$. Then, initial estimate of SC energy ($E^{i}_{sc}(t)$) corresponding to $P^{i}_{sc}(t)$ is calculated as given in (29),

$$E^{i}_{sc}(t) = E_{sc}(t-1) - \frac{P^{i}_{sc}(t)}{T_r}. \tag{29}$$

Now, SC power is considered equal to $P^{i}_{sc}(t)$ if $E^{i}_{sc}(t) \leq E_{scl}$, otherwise it is considered such that $E_{sc}(t)$ becomes equal to E_{scl} as given in (30),

$$\begin{aligned} P_{sc}(t) &= P^{i}_{sc}(t), E^{i}_{sc}(t) \leq E_{scl} \\ &= (E_{sc}(t-1) - E_{scl}) \times T_r, E^{i}_{sc}(t) > E_{scl}. \end{aligned} \tag{30}$$

B. SC Power During Charging

The SC is charged when net load forecast error is less than or equal to zero. Firstly an initial estimate of SC power is determined considering energy storage and rated power constraints as given in (31),

$$\begin{aligned} P^{i}_{sc}(t) &= 0, E_{sc}(t-1) = E_{scu} \\ &= -P_{scr}, E_{sc}(t-1) \neq E_{scu} \&\& -P_{nlfe}(t) > P_{scr} \\ &= P_{nlfe}, E_{sc}(t-1) \neq E_{scu} \&\& -P_{nlfe}(t) \leq P_{scr}. \end{aligned} \tag{31}$$

It means that if the available energy in SC is at its upper limit, the SC is not charged. Otherwise, it is charged either by P_{scr} if $-P_{nlfe}(t) > P_{scr}$ or by $P_{nlfe}(t)$ if $-P_{nlfe}(t) \leq P_{scr}$. Now, $E^{i}_{sc}(t)$ is calculated using (29). Then SC power is considered equal to $P^{i}_{sc}(t)$ if $E^{i}_{sc}(t) \leq E_{scl}$, otherwise it is considered

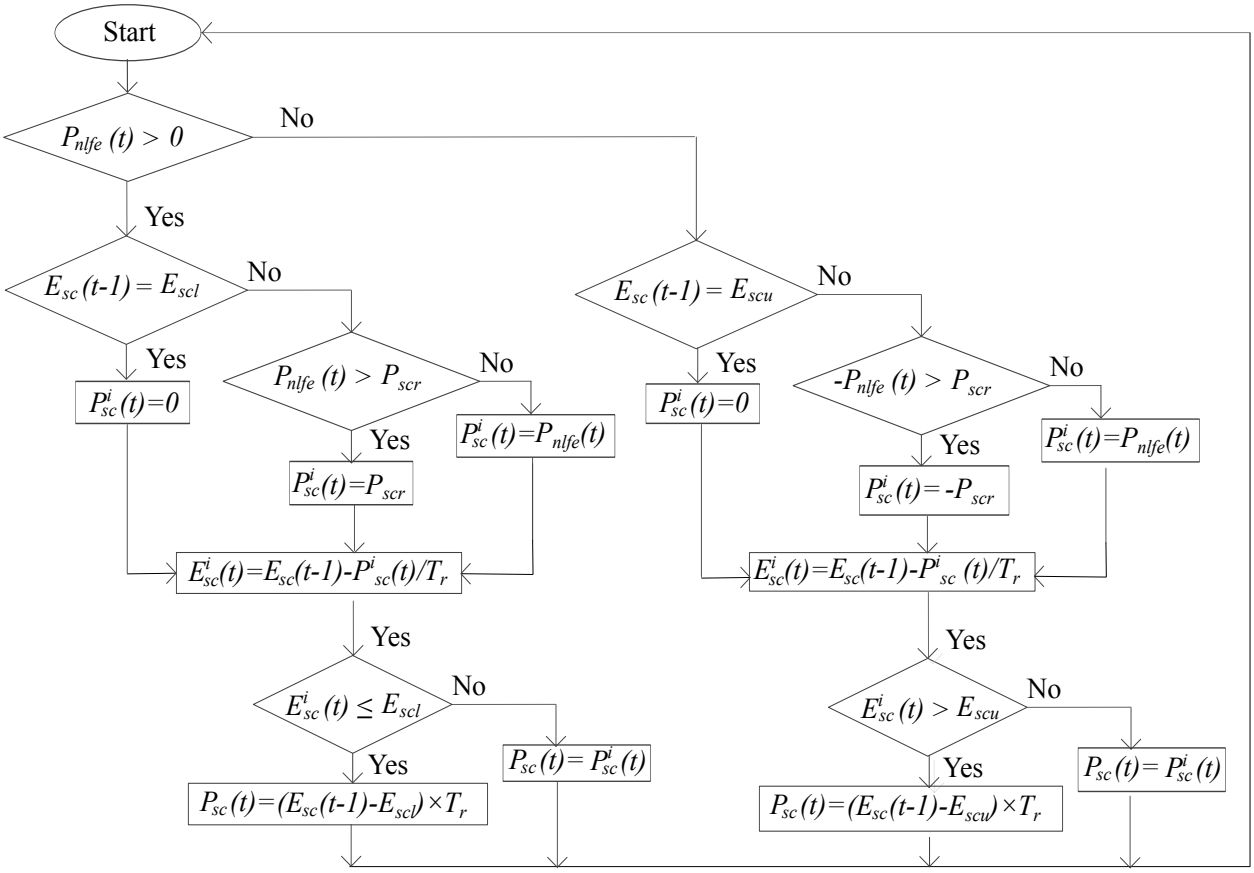

Fig. 6. Proposed control of SC for net load forecast error compensation.

such that $E_{sc}(t)$ becomes equal to E_{scu} as given in (32),

$$\begin{aligned} P_{sc}(t) &= P^i_{sc}(t), E^i_{sc}(t) \le E_{scu} \\ &= (E_{sc}(t-1) - E_{scu}) \times T_r, E^i_{sc}(t) > E_{scu}. \end{aligned} \tag{32}$$

V. Simulation Results and Discussion

The proposed method is tested for two different cases i.e., when there is more net load power over a day and less net load power over a day using MATLAB on a 64-bit operating system PC with a processor of Intel(R) Core(TM) i5-6500 CPU @ 3.2 GHz. The simulation parameters are shown in Table III. The forecast errors in the load and PV power profiles are considered to be following normal distribution. The mean values are taken as nominal forecast values. Standard deviations are taken as one-third of maximum forecast ranges. The forecast error ranges of load power and PV power are $\pm 10\%$ and $\pm 25\%$ of nominal values, respectively [33].

A. Case 1: High Peak Load and High Peak PV Power

In this case peak load power forecast is considered as 100 kW and peak PV power forecast is considered to be equal to 100 kW which are the rated load and PV source installed powers respectively. Fig. 7 shows the day-ahead and real time net load powers with forecast errors.

TABLE III
Simulation parameters [33], [34]

Parameter	Value	Parameter	Value
η_{bc}	0.95	SoC_{bl}/SoC_{bu}	0.2/0.9
η_{bd}	0.95	SoC_{b-i}	0.5
E_{br}	400 kWh	P^l_{bc}	100 kW
V_{br}	120 V	P^l_{bd}	100 kW
E_{scr}	3 kWh	SoC_{scl}/SoC_{scu}	0.49/0.98
V_{scr}	150 V	SoC_{sc-i}	0.5
C_{sc}	960 F	P_{scr}	35 kW
P_{l-r}	100 kW	P_{pv-in}	100 kW

1) Battery Power: For these day-ahead load and PV power profiles, the rule-based peak shaving method is applied and optimal DL is determined using GA. The best fitness values plot for different runs of GA is shown in Fig. 8 which indicates that the optimal DL is equal to 65.99 kW. The control inputs corresponding to this optimal DL i.e., E^o_{bc}, E^o_{nlfc}, E^o_{gc} and C^o_g are calculated as 159.84 kWh, 126.95 kWh, 981.62 kWh and 0.03, respectively. The optimal battery powers which are obtained using proposed rules over a day are shown in Fig. 9(a). It indicates that their powers are limited to the battery power limits of 100 kW.

2) SC Power: The SC powers are obtained using proposed net load forecast error compensation method and shown in Fig. 9(b). This profile indicates that their powers are limited to the rated power of 35 kW.

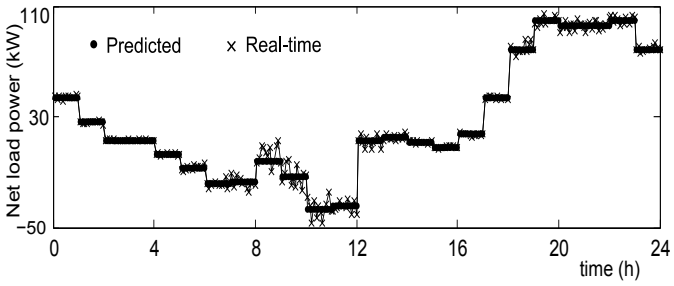

Fig. 7. Net load power in Case 1.

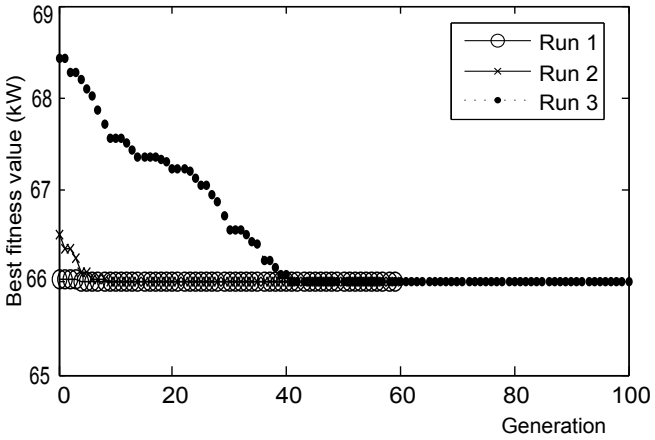

Fig. 8. Best fitness values for Case 1.

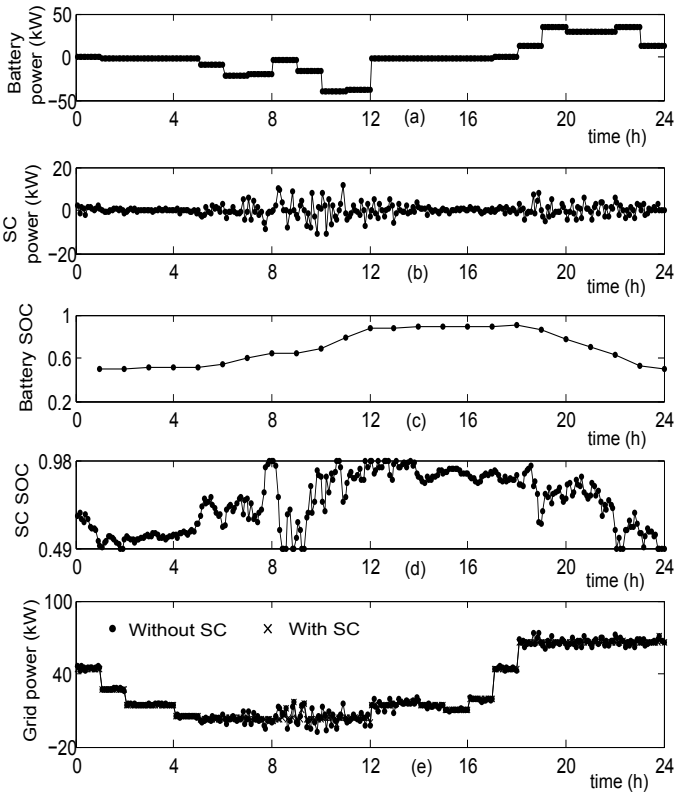

Fig. 9. Case 1. (a) Battery power. (b) SC power. (c) Battery SoC. (d) SC SoC. (e) Grid power.

3) SoC of Battery and SC: The battery SoC is indicated in Fig. 9(c). It indicates that the battery SoC is within its limits of 0.2 and 0.9. At the end of the day SoC is equal to the initial SoC of 0.5 which ensures flexible day to day management of battery. Further, SoC of SC is indicated in Fig. 9(d) which shows that SoC is within its limits of 0.49 and 0.98.

4) Grid Power: The resulting grid power is determined using (33),

$$P_g(t) + P_b(t) + P_{sc} = P_{nl}(t). \tag{33}$$

This grid power with and without SC is shown in Fig. 9(e). Without forecast errors, the peak grid demand should be limited to P^o_{dl} of 65.99 kW and there should not be any grid feed-in power as per the optimal rule-based peak shaving algorithm. However, due to forecast errors the grid peak demand and feed-in powers are 73.96 kW and 7.65 kW, respectively without SC. Further, the peak grid demand and feed-in powers with SC are 71.03 kW and 1.27 kW, respectively. Note that this peak grid demand is not same as that of the peak grid demand when there are no forecast errors i.e., 65.99 kW. Moreover, there is peak feed-in power of 1.27 kW whereas there is no feed-in power in case of no forecast errors. It means that the SC is unable to compensate forecast errors fully due to its SoC and rated power constraints.

B. Case 2: Low Peak Load and High Peak PV Power

In this case peak load power forecast is considered as 100 kW and peak PV power forecast is considered to be equal to 50 kW which are the rated load and half of the PV source installed powers respectively. Fig. 10 shows the day-ahead and real time net load powers with forecast errors.

1) Battery Power: For these day-ahead load and PV power profiles, the rule-based peak shaving method is applied and optimal DL is determined as 65.99 kW. The control inputs corresponding to this optimal DL i.e., i.e., P^o_{dl}, E^o_{bc}, E^o_{nlfc}, and P^o_{fil} are 21.58 kW, 151.52 kWh, 303.48 kWh, and 19.74 kW, respectively. The available grid energy and coefficient of grid energy to charge the battery (E^o_{gc} and C^o_g) are not applicable as $E^o_{pvc} > E^o_{bc}$. The optimal battery powers which are obtained using proposed rules over a day are shown in Fig. 11(a). It indicates that their powers are limited to the battery power limits of 100 kW.

2) SC Powers: The SC powers are obtained using proposed SC control as shown in Fig. 11(b). It shows that SC powers are limited to its rated power.

3) SoC of Battery and SC: The battery SoC is indicated in Fig. 11(c). It shows that the SoC is maintained within its limits of 0.2 and 0.9. Moreover, at the end of the day SoC is equal to the initial SoC of 0.5 which ensures the flexible day to day management. Further, SoC of SC is shown in Fig. 11(d). It indicates that the SoC is maintained within the limits of 0.49 and 0.98.

4) Grid Powers: The grid power is indicated in Fig. 11(e). Without forecast errors, the peak grid demand should be limited to P^o_{dl} of 21.58 kW and P^o_{fil} of 19.74 kW respectively which are obtained through optimal rule-based peak shaving algorithm. However, due to forecast errors the grid peak demand and feed-in powers are 25.59 kW and 28.50

kW, respectively without SC. Further, the peak grid demand and feed-in powers with SC are 21.58 kW and 23.36 kW, respectively. Note that even though this peak grid demand is same as that of the peak grid demand when there are no forecast errors, the peak feed-in power is not equal to the peak feed-in power when there are no forecast errors i.e., 19.74 kW. This is due to the SC SoC and rated power constraints.

C. Performance Comparison

The performance of the proposed forecast error compensation is presented by considering the peak grid demand and feed-in power as performance indicators. The P_{gd-p} and P_{gf-p} are determined as follows.

$$\begin{aligned} P_{gd-p} &= \text{maximum}(P_{gd}(t)) \\ P_{gf-p} &= \text{minimum}(P_{gf}(t)). \end{aligned} \tag{34}$$

In (34), the $P_{gd}(t)$ and $P_{gf}(t)$ are determined using (35) and (36), respectively.

$$\begin{aligned} P_{gd}(t) &= P_g(t),\ P_g(t) > 0 \\ &= 0,\ \text{otherwise}. \end{aligned} \tag{35}$$

$$\begin{aligned} P_{gf}(t) &= P_g(t),\ P_g(t) < 0 \\ &= 0,\ \text{otherwise}. \end{aligned} \tag{36}$$

The P_{gd-p} and P_{gd-p} must be less for better peak shaving operation. he performance of proposed method is compared with respect to the case when there is no forecast error compensation i.e. when the SC is not used. Eventhough the result analysis is discussed for two cases considering the forecast error ranges of load and PV power profiles as $\pm 10\%$ and $\pm 25\%$ of nominal values, respectively, the performance comparison is presented for other values of forecast error ranges as well as discussed follows and given in Table IV.

1) For R_{lfe}=10%, R_{pvfe}=25%: For these forecast error ranges, the results analysis is discussed and it is observed that the grid peak demand and feed-in powers are reduced by 3.96% and 83.37%, respectively with SC as compared to the case of without SC in Case 1. Similarly, the peak demand and feed-in powers are reduced by 15.67% and 18.04%, respectively with SC as compared to the case of without SC in Case 2.

2) For R_{lfe}=5%, R_{pvfe}=12.5%: For these forecast error ranges, it is found that the grid peak demand and feed-in powers in Case 1 without SC are 69.45 kW and 6.36 kW respectively. The grid peak demand and feed-in powers in Case 1 with SC are 65.9 kW and 0 kW, respectively. It indicates that the peak demand and feed-in powers are reduced by 5.11% and 100%, respectively with SC as compared to the case of without SC in Case 1.

Further, the grid peak demand and feed-in powers in Case 2 without SC are 22.98 kW and 24.55 kW respectively. The grid peak demand and feed-in powers in Case 2 with SC are 21.58 kW and 19.25 kW, respectively. It indicates that the peak demand and feed-in powers are reduced by 6.09% and 21.59%, respectively with SC as compared to the case of without SC in Case 2.

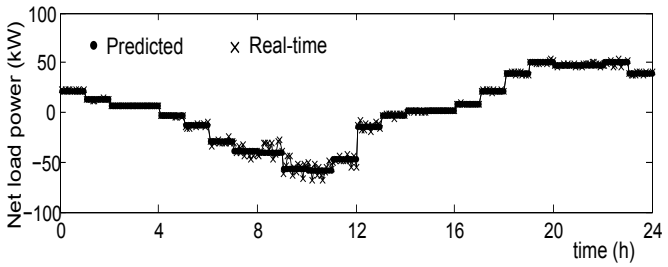

Fig. 10. Net load power in Case 2.

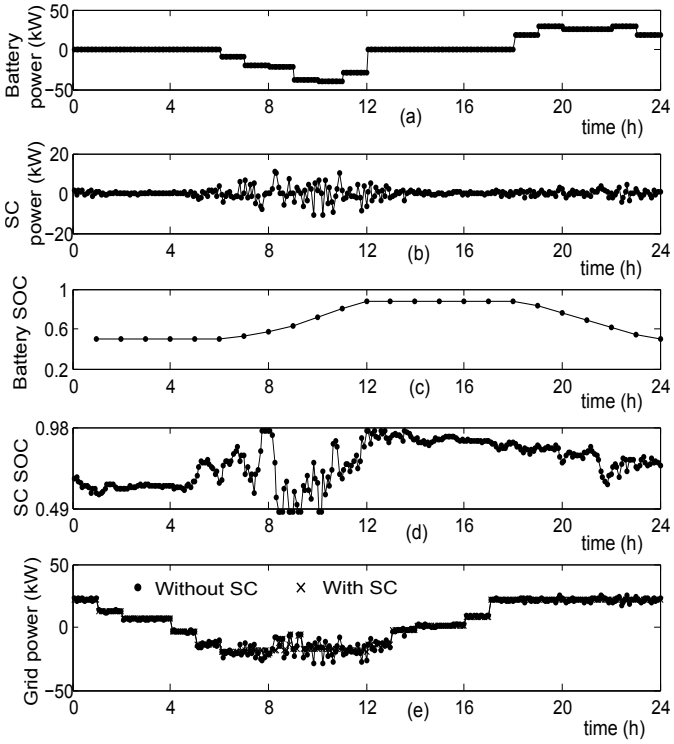

Fig. 11. Case 2. (a) Battery power. (b) SC power. (c) Battery SoC. (d) SC SoC. (e) Grid power.

D. Scalability and Challenges

Even though a smaller system is considered in this article to test the performance of proposed method, both generating source and energy storage device are present at the PCC of the system. In modern power systems without any loss of generality any node or point of common coupling (PCC) can be represented as a point where a generating source (e.g. renewable energy source) and energy storage system is connected. It means the proposed method can be extended to apply in the large power systems where there is a presence of generating source and energy storage at any point in the power systems.

Further, the proposed net load forecast error compensation method is implemented through SC which does not need any optimization problem to be solved. The SC schedules are determined using the net load power inputs at each time. Therefore it is easy to apply this method for implementing the energy management applications in real-time to reduce the impact of forecast errors. However, the main challenges

TABLE IV
PERFORMANCE COMPARISON

Case	P_{gd-p} (kW) R_{lfe}=10%, R_{pvfe}=25%		P_{gf-p} (kW) R_{lfe}=10%, R_{pvfe}=25%		P_{gd-p} (kW) R_{lfe}=5%, R_{pvfe}=12.5%		P_{gf-p} (kW) R_{lfe}=5%, R_{pvfe}=12.5%	
	without SC [31]	Proposed method	without SC [31]	Proposed method	without SC [31]	Proposed method	without SC [31]	Proposed method
Case 1	73.96	71.03	7.65	1.27	69.45	65.9	6.36	0
Case 2	25.59	21.58	28.50	23.36	22.98	21.58	24.55	19.25

of implementing the proposed method in real time are associated with the measurement and communication requirements. Because, the real time data is required to be sent to the energy management system to provide the battery and SC power references as per the proposed methods to the respective converters. If the communication failure or measurement device damage occurs, the desired performance of the proposed methods may not achieved. Further, the design of SC for optimal net load forecast error compensation is another challenge which is considered as the future scope of this work.

VI. CONCLUSIONS

The proposed net load forecast error compensation is tested in MATLAB for different cases. During high peak load and high peak PV power, the grid peak demand and feed-in power reductions in the range of 3.96% to 5.11% and 83.37%-100% are achieved, respectively with SC as compared to the case of without SC. During low peak load and high peak PV power, the grid peak demand and feed-in power reductions in the range of 6.09% to 15.67% and 18.04% to 21.59% are achieved, respectively with SC as compared to the case of without SC. The reduced peak demand provides less energy costs when time of use energy price is applied to the energy consumption cost. Moreover, reduced peak demand and feed-in powers mitigate the voltage drop and voltage rise issues, respectively when connected in the low voltage distribution systems. Further, since the forecast errors are compensated by SC, the battery life time will be improved.

REFERENCES

[1] J. Choi, J.-I. Lee, I.-W. Lee, and S.-W. Cha, "Robust PV-BESS Scheduling for a Grid With Incentive for Forecast Accuracy," *IEEE Trans. Sustain. Energy*, vol. 13, no. 1, pp. 567–578, 2022.

[2] K. Mahmud, J. Ravishankar, M. J. Hossain, and Z. Y. Dong, "The Impact of Prediction Errors in the Domestic Peak Power Demand Management," *IEEE Trans Ind. Inform.*, vol. 16, no. 7, pp. 4567–4579, 2020.

[3] Y.-R. Lee, H.-J. Kang, and M.-K. Kim, "Optimal Operation Approach With Combined BESS Sizing and PV Generation in Microgrid," *IEEE Access*, vol. 10, pp. 27 453–27 466, 2022.

[4] S. Chapaloglou, E. Alves, V. Trovato, and E. Tedeschi, "Optimal Energy Management in Autonomous Power Systems With Probabilistic Security Constraints and Adaptive Frequency Control," *IEEE Trans. Power Syst.*, pp. 1–12, 2023, doi:10.1109/TPWRS.2023.3236378.

[5] D. A. Halamay, T. K. A. Brekken, A. Simmons, and S. McArthur, "Reserve requirement impacts of large-scale integration of wind, solar, and ocean wave power generation," *IEEE Trans. Sustain. Energy*, vol. 2, no. 3, pp. 321–328, 2011.

[6] E. Ela and M. O'Malley, "Studying the variability and uncertainty impacts of variable generation at multiple timescales," *IEEE Trans. Power Syst.*, vol. 27, no. 3, pp. 1324–1333, 2012.

[7] A. Turk, Q. Wu, and M. Zhang, "Model predictive control based real-time scheduling for balancing multiple uncertainties in integrated energy system with power-to-x," *Int. J. Electr. Power Energy Syst.*, vol. 130, p. 107015, 2021.

[8] B. B. Ustundag and A. Kulaglic, "High-Performance Time Series Prediction With Predictive Error Compensated Wavelet Neural Networks," *IEEE Access*, vol. 8, pp. 210 532–210 541, 2020.

[9] X. Yang, Y. Zhang, H. He, S. Ren, and G. Weng, "Real-Time Demand Side Management for a Microgrid Considering Uncertainties," *IEEE Trans. Smart Grid*, vol. 10, no. 3, pp. 3401–3414, 2019.

[10] T. K. A. Brekken, A. Yokochi, A. von Jouanne, Z. Z. Yen, H. M. Hapke, and D. A. Halamay, "Optimal energy storage sizing and control for wind power applications," *IEEE Trans. Sustain. Energy*, vol. 2, no. 1, pp. 69–77, 2011.

[11] X. Yu, X. Dong, S. Pang, L. Zhou, and H. Zang, "Energy storage sizing optimization and sensitivity analysis based on wind power forecast error compensation," *Energies*, vol. 12, no. 24, 2019.

[12] H. Bludszuweit and J. A. Dominguez-Navarro, "A probabilistic method for energy storage sizing based on wind power forecast uncertainty," *IEEE Trans. Power Syst.*, vol. 26, no. 3, pp. 1651–1658, 2011.

[13] P. Mathew, S. Madichetty, and S. Mishra, "A multilevel distributed hybrid control scheme for islanded dc microgrids," *IEEE Syst. J.*, vol. 13, no. 4, pp. 4200–4207, 2019.

[14] A. Aktas, K. Erhan, S. Ozdemir, and E. Ozdemir, "Experimental investigation of a new smart energy management algorithm for a hybrid energy storage system in smart grid applications," *Electr. Power Syst. Res.*, vol. 144, pp. 185–196, 2017.

[15] C. R. Lashway, A. T. Elsayed, and O. A. Mohammed, "Hybrid energy storage management in ship power systems with multiple pulsed loads," *Electr. Power Syst. Res.*, vol. 141, pp. 50–62, 2016.

[16] J. R. Rani, R. Thangavel, M. Kim, Y. S. Lee, and J.-H. Jang, "Ultra-high energy density hybrid supercapacitors using mno2/reduced graphene oxide hybrid nanoscrolls," *Nanomaterials*, vol. 10, no. 10, 2020.

[17] M. G. Damavandi, J. R. Martí, and V. Krishnamurthy, "A methodology for optimal distributed storage planning in smart distribution grids," *IEEE Trans.Sustain. Energy*, vol. 9, no. 2, pp. 729–740, 2018.

[18] Y. Ding, Q. Xu, and Y. Huang, "Optimal sizing of user-side energy storage considering demand management and scheduling cycle," *Electr. Power Syst. Res.*, vol. 184, p. 106284, 2020.

[19] S. L. Arun and M. P. Selvan, "Intelligent residential energy management system for dynamic demand response in smart buildings," *IEEE Syst. J.*, vol. 12, no. 2, pp. 1329–1340, 2018.

[20] K. A. Joshi, N. M. Pindoriya, and A. K. Srivastava, "A two-stage fuzzy multiobjective optimization for phase-sensitive day-ahead dispatch of battery energy storage system," *IEEE Syst. J.*, vol. 12, no. 4, pp. 3649–3660, 2018.

[21] S. Zhao, X. Lin, and M. Chen, "Robust Online Algorithms for Peak-Minimizing EV Charging Under Multistage Uncertainty," *IEEE Trans. Automat. Contr.*, vol. 62, no. 11, pp. 5739–5754, 2017.

[22] N. Chakraborty, A. Mondal, and S. Mondal, "Efficient Scheduling of Nonpreemptive Appliances for Peak Load Optimization in Smart Grid," *IEEE Trans. Ind. Informat.*, vol. 14, no. 8, pp. 3447–3458, 2018.

[23] Y. Mo, Q. Lin, M. Chen, and S. J. Qin, "Optimal Peak-Minimizing Online Algorithms for Large-Load Users with Energy Storage," in *IEEE INFOCOM 2021 -IEEE Conf. Comput. Commun. Workshops (INFOCOM WKSHPS)*, 2021, pp. 1–2.

[24] Y. Guo, Q. Zhang, and Z. Wang, "Cooperative Peak Shaving and Voltage Regulation in Unbalanced Distribution Feeders," *IEEE Trans. Power Syst.*, vol. 36, no. 6, pp. 5235–5244, 2021.

[25] K. Mahmud, M. J. Hossain, and G. E. Town, "Peak-Load Reduction by Coordinated Response of Photovoltaics, Battery Storage, and Electric Vehicles," *IEEE Access*, vol. 6, pp. 29 353–29 365, 2018.

[26] D. M. Greenwood, N. S. Wade, P. C. Taylor, P. Papadopoulos, and N. Heyward, "A Probabilistic Method Combining Electrical Energy Storage and Real-Time Thermal Ratings to Defer Network Reinforcement," *IEEE Trans. Sustain. Energy*, vol. 8, no. 1, pp. 374–384, 2017.

[27] D. T. Vedullapalli, R. Hadidi, and B. Schroeder, "Combined HVAC and

Battery Scheduling for Demand Response in a Building," *IEEE Trans. Ind. Appl.*, vol. 55, no. 6, pp. 7008–7014, 2019.
[28] N. Ahmed, M. Levorato, and G. P. Li, "Residential Consumer-Centric Demand Side Management," *IEEE Trans. Smart Grid*, vol. 9, no. 5, pp. 4513–4524, 2018.
[29] von Appen, Jan and Stetz, Thomas and Braun, Martin and Schmiegel, Armin, "Local Voltage Control Strategies for PV Storage Systems in Distribution Grids," *IEEE Trans. Smart Grid*, vol. 5, no. 2, pp. 1002–1009, 2014.
[30] R. Manojkumar, C. Kumar, S. Ganguly, and J. P. S. Catalão, "Optimal peak shaving control using dynamic demand and feed-in limits for grid-connected pv sources with batteries," *IEEE Syst. J.*, vol. 15, no. 4, pp. 5560–5570, 2021.
[31] R. Manojkumar, C. Kumar, S. Ganguly, H. B. Gooi, S. Mekhilef, and J. P. S. Catalx00E3;o, "Rule-based peak shaving using master-slave level optimization in a diesel generator supplied microgrid," *IEEE Trans. Power Syst.*, vol. 38, no. 3, pp. 2177–2188, 2023.
[32] "IEEE Standard for the Specification of Microgrid Controllers," *IEEE Std 2030.7-2017*, pp. 1–43, 2018.
[33] R. Manojkumar, C. Kumar, and S. Ganguly, "Optimal demand response in a residential pv storage system using energy pricing limits," *IEEE Trans. Ind. Informat.*, vol. 18, no. 4, pp. 2497–2507, 2022.
[34] O. Salari, K. H. Zaad, A. Bakhshai, and P. Jain, "Reconfigurable hybrid energy storage system for an electric vehicle dc–ac inverter," *IEEE Trans. Power Electron.*, vol. 35, no. 12, pp. 12 846–12 860, 2020.

Rampelli Manojkumar (Member, IEEE) Rampelli Manojkumar received the B.E. degree in electrical and electronics engineering from the Vasavi College of Engineering, Hyderabad, India, in 2013, and the M.Tech. degree in power and energy systems from the National Institute of Technology Karnataka, Surathkal, India, in 2015. He has obtained the Ph.D. degree from the Department of Electronics and Electrical Engineering, Indian Institute of Technology Guwahati.

He is currently working as the Assistant Professor in the department of Electrical and Electronics Engineering, BVRIT HYDERABAD College of Engineering for Women. His research interests include energy management, optimal power flow, hybrid ac/dc distribution systems. He is the Speaker of IEEE Smart Grid webinar. He is the reviewer of IEEE Transactions on Industrial Informatics, IEEE Systems Journal, IEEE Access, Applied Energy, Energy Reports, and International Journal of Electrical Power and Energy Systems.

Chandan Kumar (Senior Member, IEEE) received the B.Sc. degree from the Muzaffarpur Institute of Technology, Muzaffarpur, India, in 2009, the M.Tech. degree from the National Institute of Technology, Trichy, India, in 2011, and the Ph.D. degree from the Indian Institute of Technology Madras, Chennai, India, in 2014, all in electrical engineering.

Since 2015, he has been an Assistant Professor with the Electronics and Electrical Engineering Department, Indian Institute of Technology Guwahati, Guwahati, India. During 2016 to 2017, he was an Alexander von Humboldt Research Fellow with the Chair of Power Electronics, University of Kiel, Kiel, Germany. His research interests include power electronics application in power system, power quality, and renewable energy. He is serving as Associate Editor of IEEE Systems Journal, IEEE Open Journal of Power Electronics, IEEE Open Journal of the Industrial Electronics Society (OJIES), and IEEE Access Journal.

Sanjib Ganguly (Senior Member, IEEE) was born in 1981 in India. He received the B.E. and M.E. degrees in electrical engineering from Indian Institute of Engineering Science and Technology, Shibpur, India and Jadavpur University, India in 2003 and 2006, respectively. He received the Ph.D degree from Indian Institute of Technology Kharagpur, India in 2011.

He is presently working as Associate Professor in the Department of Electronics and Electrical Engineering in Indian Institute of Technology Guwahati, India. His research interest includes power system operation and planning, custom power devices, hybrid energy system, and evolutionary algorithms.

João P. S. Catalão (Fellow, IEEE) received the M.Sc. degree from the Instituto Superior Técnico (IST), Lisbon, Portugal, in 2003, and the Ph.D. degree and Habilitation for Full Professor (quot;Agregaçãoquot;) from the University of Beira Interior (UBI), Covilha, Portugal, in 2007 and 2013, respectively. Currently, he is a Professor at the Faculty of Engineering of the University of Porto (FEUP), Porto, Portugal. He was the Primary Coordinator of the EU-funded FP7 project SiNGULAR, a 5.2-million-euro project involving 11 industry partners. He has authored or coauthored more than 500 journal publications and 400 conference proceedings papers, with an h-index of 89 and more than 30,000 citations (according to Google Scholar), having supervised more than 120 post-docs, Ph.D. and M.Sc. students, and other students with project grants. He was the General Chair and General Co-Chair of SEST 2019 and SEST 2020, respectively, after being the inaugural Technical Chair and co-founder of SEST 2018. He is a Senior Editor of the IEEE TRANSACTIONS ON NEURAL NETWORKS AND LEARNING SYSTEMS. Furthermore, he is an Associate Editor of nine other IEEE TRANSACTIONS/JOURNALS. He was an IEEE Computational Intelligence Society (CIS) Fellows Committee Member in 2022 and 2023. He was recognized as one of the Outstanding Associate Editors 2020 of the IEEE TRANSACTIONS ON SMART GRID, and one of the Outstanding Associate Editors 2021 of the IEEE TRANSACTIONS ON POWER SYSTEMS. He has multiple Highly Cited Papers in Web of Science. He has won 5 Best Paper Awards at IEEE Conferences. Furthermore, he was the recipient of the 2017-2022 (for the sixth consecutive year) FEUP Scientific Recognition Diplomas. His research interests include power system operations and planning, power system economics and electricity markets, distributed renewable generation, demand response, smart grid, and multi-energy carriers.